

RAMAN SPECTROSCOPIC STUDY OF ION-IMPLANTED AND ANNEALED SILICON.

David. D. Tuschel*, James P. Lavine**, and Jeffrey B. Russell**

*Imaging Research and Advanced Development
Eastman Kodak Company, Rochester, NY 14650-2017

**Microelectronics Technology Division
Eastman Kodak Company, Rochester, NY 14650-2008

ABSTRACT

Raman spectroscopy is used to characterize silicon implanted with arsenic and then annealed. The implant dose ranged from 2×10^{12} to $2 \times 10^{13}/\text{cm}^2$. The as-implanted samples show a decreased Raman intensity of the 520 cm^{-1} optical mode, and increased Raman intensity between 400 and 500 cm^{-1} with respect to an unimplanted silicon wafer. The higher arsenic doses show an increase in the second-order transverse acoustic-mode (TA) intensity around 300 cm^{-1} relative to the second-order transverse optical-mode (TO) intensity near 970 cm^{-1} . Annealing restores the $2\text{TA}/2\text{TO}$ relative intensities and sharpens the weak peaks between 600 and 900 cm^{-1} . The Raman spectrum is altered by the lowest dose implant and the annealing steps do not lead to a complete recovery of the pre-implant Raman spectrum. This permits the monitoring of low-dose ion-implant damage recovery with Raman spectroscopy.

INTRODUCTION

Ion implantation continues to play a dominant role in the fabrication of semiconductor devices. Hence, there is an ongoing need to monitor low-dose implants in order to measure the degree of damage and to detail the effects of thermal annealing. The ideal characterization method involves minimal sample preparation and provides results quickly. Since Raman spectroscopy meets these criteria, it is evaluated here for low-dose arsenic implantation into silicon.

Previous work with xenon-implanted GaAs [1] established that implant doses just below $10^{12}/\text{cm}^2$ produced changes in the Raman spectrum. Huang and collaborators [2,3] demonstrated that silicon implants into silicon start to alter the Raman spectrum when the dose exceeds 10^{12} Si atoms/ cm^2 . Othonos et al. [4] used Raman spectroscopy to study the annealing of phosphorus-implanted silicon at doses of $10^{13}/\text{cm}^2$ and

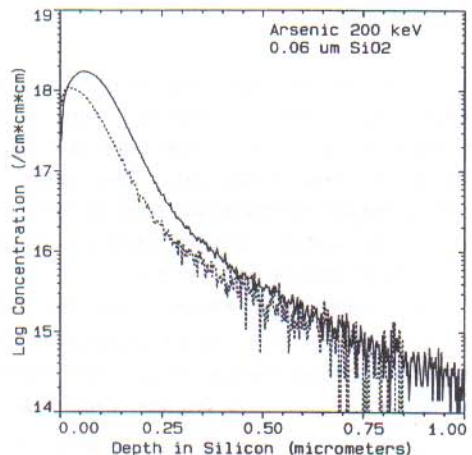
greater. Balkanski et al. [5] reported Raman spectra for arsenic doses in silicon of 10^{14} and $10^{16}/\text{cm}^2$, which produce an amorphous region in the silicon. The present work also examines arsenic-implanted silicon, but the dose is only $2 \times 10^{12}/\text{cm}^2$ to $2 \times 10^{13}/\text{cm}^2$. The spectra of as-implanted silicon are compared to those of unimplanted silicon and implanted and annealed silicon. The Raman spectra provide evidence of the implant and of the annealing. Thus, Raman spectroscopy is able to monitor low-dose arsenic implants.

The second section describes the sample preparation and the Raman measurements. The third section contains the measured data and the final section discusses the experimental results.

EXPERIMENTAL PROCEDURES

Lightly-doped, p-type, $\langle 100 \rangle$ silicon wafers were implanted with 200 keV arsenic ions through a $0.06\text{-}\mu\text{m}$ thick thermal oxide. Selected wafers then received a 15 second rapid thermal anneal (RTA) at 1125°C . Other wafers were oxidized in a furnace at 950°C and then oxidized a second time after a complete etchback of the silicon dioxide. The second oxidation grew $0.05\ \mu\text{m}$ of SiO_2 at 950°C . Each oxidation included nitrogen annealing steps at 950°C . There are as-implanted, RTA, and furnace-annealed samples for each implant dose. Figure 1 shows secondary ion mass spectrometry (SIMS) profiles of the as-implanted and furnace-annealed samples for the $2 \times 10^{13}\ \text{As}/\text{cm}^2$ case. The RTA profile

Fig. 1. SIMS profiles of 200 keV arsenic-implanted (solid line) and furnace annealed (dashed line) Si. Dose is $2 \times 10^{13}/\text{cm}^2$.



falls on the as-implanted profile, which establishes the depth scale.

The Raman spectroscopy is done with a SPEX 1403 double monochromator and 200 mW of laser excitation at 488 nm. The Raman shift spectra are obtained over 100 to 1100 cm^{-1} , and are collected in increments of 1 cm^{-1} at an integration time of 2 seconds per increment. The monochromator's entrance and exit slits are set to 400 μm , while its middle slits are set to 480 μm . The samples are held in a holder such that there is a 60° angle between the incident beam and the normal to the sample surface. A 90° geometry is used for the collection of the scattered light. An unimplanted, 10-30 Ohm-cm, n-type, $\langle 100 \rangle$ silicon wafer serves as a crystalline silicon reference. The interpretation of the Raman spectrum of silicon is discussed in Refs. [2,6-8].

RESULTS

Figures 2 and 3 present the Raman spectra for the as-implanted samples. The low-energy side of the optical phonon peak at 520 cm^{-1} gains in intensity as the implant dose is increased from 2×10^{12} to $2 \times 10^{13} \text{ As/cm}^2$. This phenomenon is associated with damaged or amorphised

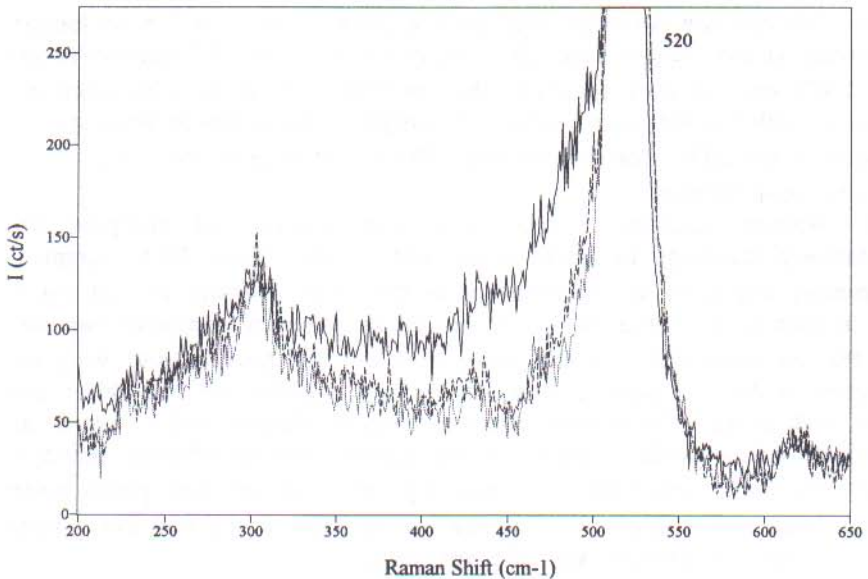


Fig. 2. Raman spectra of arsenic-implanted Si. Dose of $2 \times 10^{13}/\text{cm}^2$ (solid line), $6.8 \times 10^{12}/\text{cm}^2$ (dashed line), and $2 \times 10^{12}/\text{cm}^2$ (dottedline).

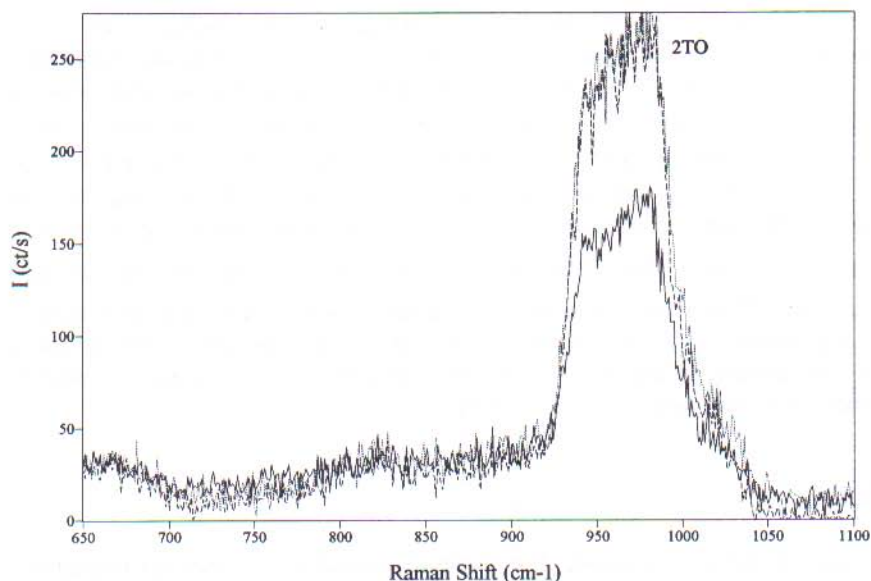


Fig. 3. Continuation of Fig. 2 to 1100 cm^{-1} . Lines are defined in Fig. 2

silicon [4,9] and the two-acoustical phonon peak at 440 cm^{-1} is no longer discernible at the highest dose [2]. The intensity of the 2TO phonon region around 970 cm^{-1} is also decreased by the implant from the 600 counts/s measured with the reference wafer. The higher arsenic doses show an increase in the 2TA intensity around 300 cm^{-1} relative to the 2TO intensity near 970 cm^{-1} .

The Raman spectra of the three furnace-annealed samples are qualitatively identical to each other and to the three RTA samples. Differences are seen in the recovery of the peak intensity at 520 cm^{-1} . This is portrayed in Fig. 4, which compares the two annealed samples with the as-implanted for the dose of $2 \times 10^{13}\text{ As/cm}^2$ and with the reference wafer. Figure 5 has the Raman spectra for the latter two cases, and for the RTA sample over the complete Raman shift range, at an expanded vertical scale. The annealing restores the two-phonon peaks at about 300 , 440 , and 970 cm^{-1} and the three two-phonon peaks seen between 600 and 900 cm^{-1} . The low-energy side of the 520 cm^{-1} peak also decreases in intensity with the annealing.

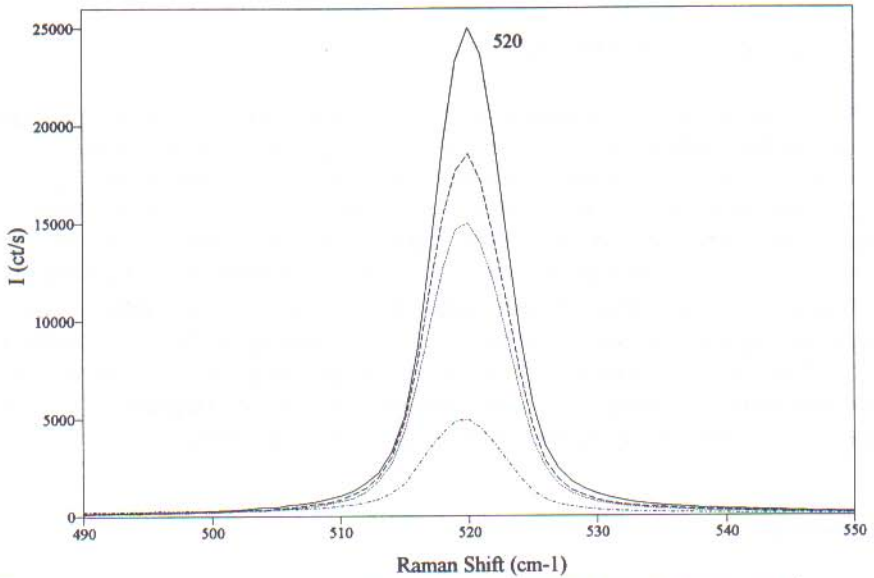


Fig. 4. Raman spectra around the optical phonon peak at 520 cm^{-1} . Reference wafer (solid line) and $2 \times 10^{13}\text{ As/cm}^2$ samples: RTA (dashed line), furnace anneal (dotted line), and as-implemented (dash-dot line).

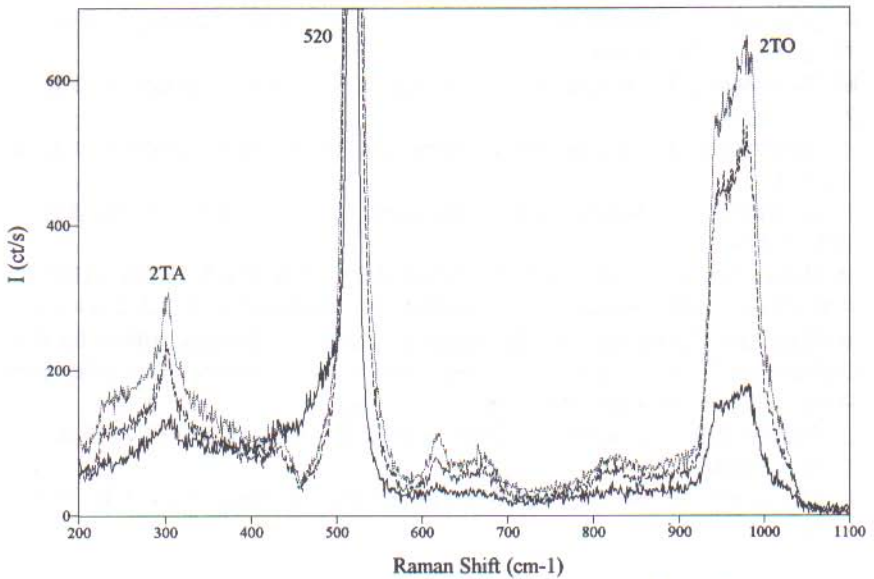


Fig. 5. Expanded Raman spectra: as-implemented $2 \times 10^{13}/\text{cm}^2$ (solid line), RTA of $2 \times 10^{13}/\text{cm}^2$ (dashed line), and reference wafer (dotted line).

DISCUSSION AND CONCLUSIONS

The previous section shows that Raman spectroscopy follows changes in the silicon wafer because of low-dose arsenic implantation. This provides a method to monitor ion implantation and annealing that utilizes simple sample preparation and provides results quickly. Raman spectroscopy shows that the implanted-ion induced damage causes the phonon peaks to decrease in intensity. Annealing restores the peaks, but the intensity of the optical phonon peak at 520 cm^{-1} shows differences in the annealing procedures. Further work is underway to find the cause of this. Possible explanations include damaged regions or clusters that resist annealing. These have been observed [3,10], or suggested [11], for higher dose implants in earlier Raman spectroscopy work.

REFERENCES

1. P.S. Peercy, *Appl. Phys. Lett.* **18**, 574 (1971).
2. X. Huang, *J. Phys. D: Appl. Phys.* **28**, 202 (1995).
3. X. Huang, F. Ninio, L.J. Brown, and S. Praver, *J. Appl. Phys.* **77**, 5910 (1995).
4. A. Othonos, C. Christofides, J. Boussey-Said, and M. Bisson, *J. Appl. Phys.* **75**, 8032 (1994).
5. M. Balkanski, J.F. Morhange, and G. Kanellis, *J. Raman Spectros.* **10**, 240 (1981).
6. K. Uchinokura, T. Sekine, and E. Matsuura, *Solid State Commun.* **11**, 47 (1972).
7. K. Uchinokura, T. Sekine, and E. Matsuura, *J. Phys. Chem. Solids* **35**, 171 (1974).
8. M. Cardona, S.C. Chen, and S. P. Varma, *Phys. Rev. B* **23**, 5329 (1981).
9. P.X. Zhang, R.D. Goldberg, I.V. Mitchell, P.J. Schultz, and D.J. Lockwood, in Materials Synthesis and Processing Using Ion Beams, edited by R.J. Culbertson, O.W. Holland, K.S. Jones, and K. Maex (*Mater. Res. Soc. Symp. Proc.* 316, Pittsburgh, PA, 1994), p. 87-92.
10. G. Braunstein, D. Tuschel, S. Chen, and S.-T. Lee, *J. Appl. Phys.* **66**, 3515 (1989).
11. K. Mizoguchi, H. Harima, and S.-i. Nakashima, *J. Appl. Phys.* **77**, 3388 (1995).